



**HAL**  
open science

## Analytical modeling and optimization of a radial permanent magnets synchronous machine

Bill Sesanga, Frédéric Wurtz, Albert Foggia

► **To cite this version:**

Bill Sesanga, Frédéric Wurtz, Albert Foggia. Analytical modeling and optimization of a radial permanent magnets synchronous machine. ISEF 2009 - XIV International Symposium on Electromagnetic Fields, Sep 2009, Arras, France. pp.371-372. hal-00419647

**HAL Id: hal-00419647**

**<https://hal.science/hal-00419647>**

Submitted on 24 Sep 2009

**HAL** is a multi-disciplinary open access archive for the deposit and dissemination of scientific research documents, whether they are published or not. The documents may come from teaching and research institutions in France or abroad, or from public or private research centers.

L'archive ouverte pluridisciplinaire **HAL**, est destinée au dépôt et à la diffusion de documents scientifiques de niveau recherche, publiés ou non, émanant des établissements d'enseignement et de recherche français ou étrangers, des laboratoires publics ou privés.

## Analytical modeling and optimization of a radial permanent magnets synchronous machine

Bill Sesanga, Frederic Wurtz and Albert Foggia

Grenoble Electrical Engineering Laboratory (G2ELAB), ENSE3 (Grenoble INP-UJF, CNRS UMR 5529)  
BP 46 -38402 Saint Martin d'Hères Grenoble Cedex, France  
bill.sesanga@g2elab.grenoble-inp.fr

**Abstract** – Nowadays, designers typically use modeling tools and numerical calculation for the electrical machine sizing, particularly the finite element method. The finite element method has been validated and has proved to be a very efficient one. However, due to problem complexity, this method is still time-consuming and large computer memory is needed. In this paper, we propose a faster analytical model (magnetic and thermal) coupled with an optimization tool CADES (Component Architecture for the Design of Engineering Systems) [1-2] to optimize a range of machines (from a few kW to more than 300 kW, and for speed ranges from 100 rpm to more than 5500 rpm). For this we used a deterministic optimization algorithm called Sequential Quadratic Programming (SQP) [3-4].

### Analytic Modeling

#### Magnetic model

Induction calculation in the air gap is the central issue in the modeling. The waveform of this induction is obtained by solving a nonlinear implicit equation system (1). The first equation of this system is directly obtained using the Ampere's theorem. To do this, the evolution of the magneto motive force (MMF) was supposed sinusoidal. The MMF amplitude, the ampere's-turns in the back iron and the polar pieces were neglected. The theorem contour is shown in Fig. 1.

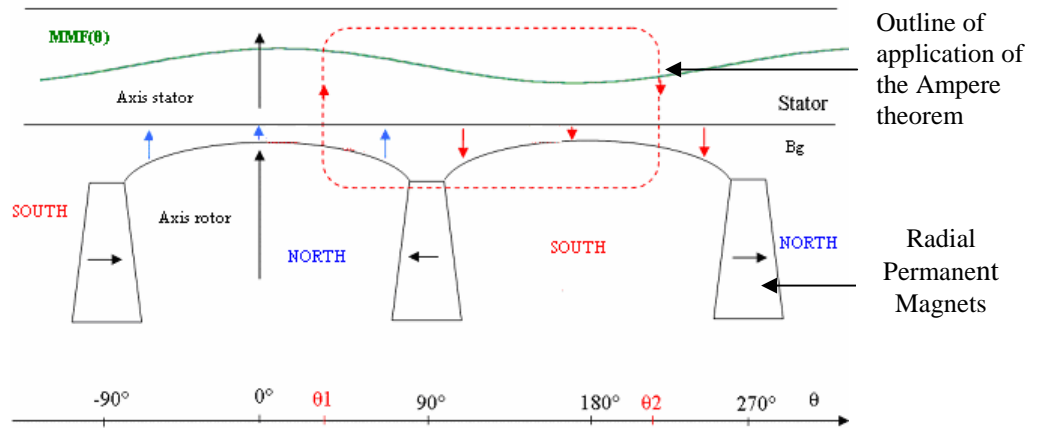


Fig. 1: Developed scheme for a poles pair and the chosen Ampere's theorem path.

The second equation of the system is obtained applying the flux conservation law.

$$\begin{cases} H_{mg} * W_{m\_mg} + \frac{2 * B_g(\theta)}{\mu_0} * \left[ g(\theta) + \frac{kt * h_{te}}{\mu(B_g(\theta))} \right] = Line\_Load * \frac{\Phi_b}{p} * \sin(\theta - \alpha) \\ \Phi_{mg}(H_{mg}) = \Phi_g(B_g(\theta)) + \Phi_f(H_{mg}) + \Phi_{f3D}(H_{mg}) \end{cases} \quad (1)$$

In this equation  $H_{mg}$  is the magnetic field in the magnets,  $W_{m,mg}$  is the minimal magnet width,  $h_{te}$  is the height of stator teeth,  $k_t$  is a geometric coefficient that allows to calculate the induction in the teeth given the air gap induction.  $B_g(\theta)$  is the air gap induction,  $g(\theta)$  is the corrected mechanic air gap,  $\theta$  is the electrical angle that could vary along a polar piece and  $\alpha$  is the auto-piloting angle.  $\Phi_b$  is the bore diameter and  $p$  the pair of poles.

All variables are calculated using the induction.  $\Phi_{mg}$  is the flux created by 2 magnets common to a pole, this flux feeds at the same time the air gap flux ( $\Phi_g$ ), the leak flux at the hub level ( $\Phi_f$ ) and the three-dimensional leak flux ( $\Phi_{f3D}$ ) in the motor edge.

### Thermal model

The integration of a thermal model was necessary because of the temperature influence on the motor materials, and most of all on permanent magnets performances. But, thermal modeling of machines is still a difficult task because of the great number of non-measurable parameters that is needed. The included model takes into account conduction and convection phenomenon but doesn't consider radiation [5].

#### Hypothesis and choice of structure of the thermal model

- By construction a motor dissipates the heat radially. Therefore, we can represent the motor with a 2D thermal finite elements model.
- The air-gap can be considered as a thermal barrier; hence rotor losses are negligible (no current, no global induction variation), which means that rotor losses will have no incidence on the temperature of winding [6].

These two hypotheses and the machine symmetries allow to use for analysis on a parts of the system as describe bellow.

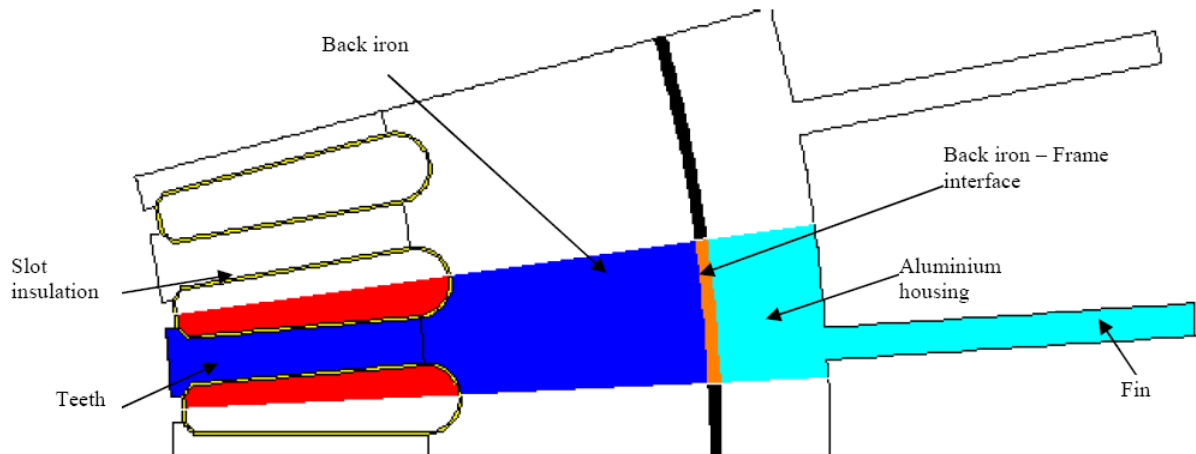


Fig. 2: Geometry used to establish the thermal model

The thermal conduction resistances are obtained by:

$$R_{th\_cond} = \frac{1}{\lambda} \frac{L}{S} \quad (2)$$

Where  $\lambda$  is the thermal conductivity of material, L the Length of the thermal flux path and S the surface crossed by the same thermal flux. The thermal convection resistance is obtained by using the Fourier's relation,  $h_{conv}$  is the exchange coefficient.

$$R_{th\_conv} = \frac{1}{h_{conv} * S} \quad (3)$$

We selected a 300 mm stator diameter machine that was fully tested on the test bench. Results were compared to the calculation and proved the reliability of the model. The thermal module of Flux2D was used to analyse temperatures in different parts of machine.

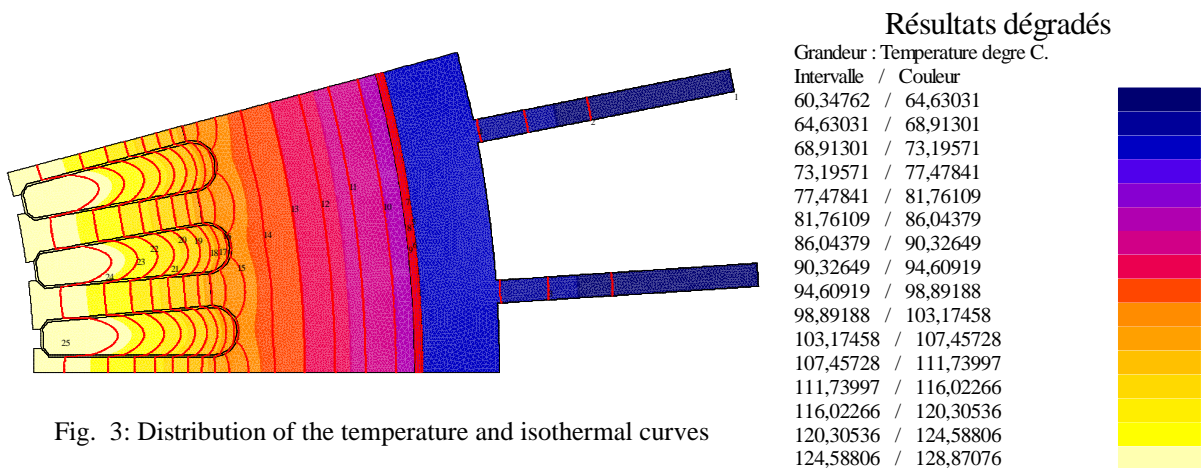


Fig. 3: Distribution of the temperature and isothermal curves

From these isothermal curves we can observe that the stream of heat follows a radial direction. Then, we modeled a network of the thermal resistances under Pspice software. In this model, copper and iron losses are considered as current sources, while temperature in each point is considered as an electrical potential, and thermal resistances are equivalent to the electrical resistances.

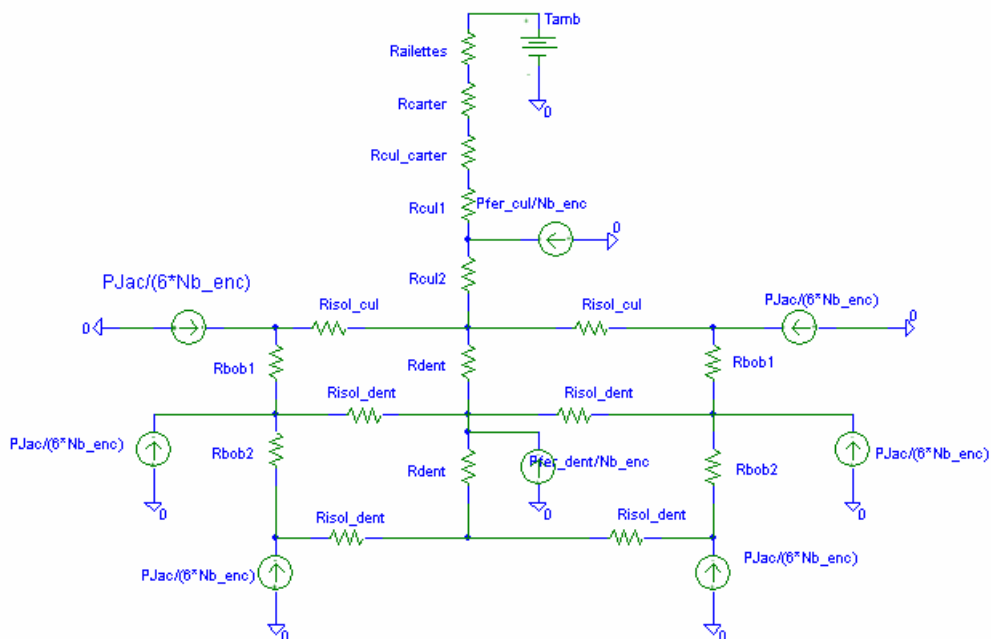


Fig. 4: Network of the thermal resistances

To validate this network of thermal resistances, we made a comparison between the FLUX2D results and Pspice. The results contained in Table1 shows that the differences between the two models are lower than 2%, which is very acceptable for a thermal model.

Node	Flux 2D Model (°C)	Pspice Model (°C)	Difference (%) In Kelvin
Ambient	20	20	0
Base fins	66.9	64.5	-0.71
Base frame	68.3	65.6	-0.79
Bore diameter	81.7	79.0	-0.76
Back iron center	90.9	88.6	-0.63
Teeth height	101.8	97.5	-1.15
Height coil	103.8	106.3	0.66
center coil	123.4	119.2	-1.06
Base coil	127.4	122.1	-1.32
Teeth center	118.0	117.4	-0.15
bottom teeth	123.4	120.1	-0.83

Table 1. Comparison temperature

### Optimizations

Before launching the optimization study, the model has been validated by comparisons with experimental tests on two machines. The first machine has a 240 mm outside diameter and 200 mm of stack length. It is a three phase PM machine with a 54 slots stator and 3 poles pair, for a nominal power of 89 kW and a rotation speed of 7200 rpm. The second machine has a 473.5 mm outside diameter and 460 mm of stack length. It is also a three phase PM machine with a 72 slots stator and 4 poles pair, for nominal power of 114 kW and a rotation speed of 700 rpm.

	Machine 1		Machine 2	
	Experimental tests	Model	Experimental tests	Model
Outside diameter (mm)	240		473.5	
Torque (N.m)	111		1504	
speed (rpm)	7199.6		701.01	
Output Power (kW)	83.6		110.4	
Input Power (kW)	89	90	114	113.9
Efficiency (%)	93.87	93.45	96.88	96.5
current (A)	194.6	195.9	175.4	177.0
Voltage (V)	341.2	328.1	399.0	399.8
Internal angle (°)	12.73	12.73	35.58	27.00

Table 2. Comparison experimental results and model

The result in Table 2 shows that the differences between tests and calculations are lower than 3%. This is totally acceptable and could be explained by both: uncertainties of measurement and calculation hypothesis (no saturation and no teeth harmonics).

### Mono objective optimization

Our model contains 25 design parameters as an input and 36 output constrained parameters. Two types of constraints can be applied to the parameters, a constraint of equality which fixes the parameter value or a constraint of disparity which determines an interval of variation. Some constraints are presented in Table 3 below.

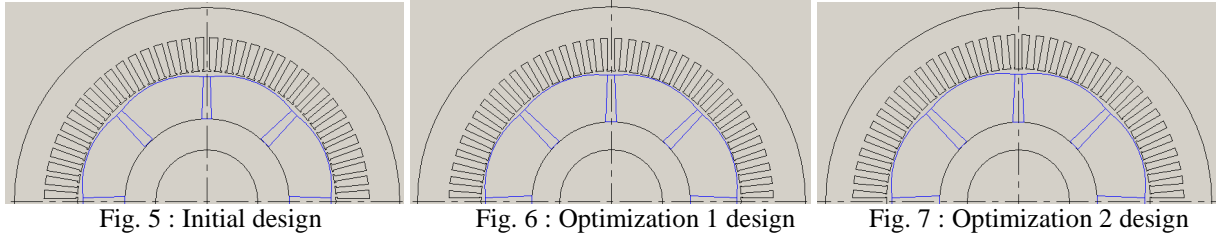
Voltage	< 340 V		Outside diameter	fixed
Induction in teeth	< 2 T		Magnetic field in magnets	< 650 kA/m
Maximal geometrical air-gap	$1,5 \cdot G_{\min} < G_{\max} < 4 \cdot G_{\min}$		Heating of the copper	< 80 °
poles number	6 or 8 according to the diameter of the machine		Slots number	3 slots /pole/phase

Table 3. Some constraints

With the SQP algorithms we have to use continuous and derivable objective and constraints [7], hence the impossibility of dealing with the specification phase for discrete variables. However, for certain variables, this problem can be addressed by treating them as continuous. This is namely the case of those variables linked to motor windings (wire diameter, number of turns ...), because the combinations are so large that it is always possible, such as adjusting a parameter or another, or the machine winding to obtain the desired voltage while respecting the geometric constraints. Unless otherwise indicated, all the parameters of the machine will be free or constrained, with the exception of the number of slots and the number of poles that will be fixed. The objective function for the optimization is the materials cost for a nominal operating point, we therefore seek to minimize this cost. Being aware that the SQP algorithm, as all deterministic type, can provide a local minimum (or maximum) of objective function, all optimizations have been validated a second time by using a genetic algorithm [8]. This assures the localization of the overall maximum, which is then refined by using the SQP algorithm. This method computing time consuming (between 10 and 20 minutes against several seconds for a single SQP) but ensures that the maximum provided by SQP is the overall maximum.

	Initial Machine	Optimization 1	Optimization 2
Materials cost (€)	405.45	366.42	364.39
Torque (N.m)	271		
Heating (Tamb=40° C)	66	66	65
Power output	85		
Voltage (V)	345.1	340	340
Current (A)	167.2	167.2	167.2
Efficiency (%)	95.9	95.9	95.9
Magnetic field in magnets (kA/m)	433	440	454
Power factor	0.905	0.917	0.918
Internal angle (°)	24.31	27.90	27.72
Cost/Torque	1.50	1.35	1.35
Torque/kg	2.53	2.76	2.76
deterministic iterations		35	33
Genetic iterations		12867	7344

Table 4. Optimizations results.



Figs. 5, 6 and 7 are graphical representations of various optimizations; optimization 1 is achieved with a fixed bore diameter and optimization 2 with a free bore diameter. The results in Table 4 clearly show that the optimized machines exhibit the same performance compared to the original machine for a lower material cost. The optimization 1 provides a gain of -9.63 % in the cost of the materials. Optimization 2 brings a more important gain of 10.13% in the cost of the materials. The power factor is improved from that of the initial machine.

### Multi objectives optimizations

The optimization presented here above leads only an optimum machine for a particular speed. But manufacturers always need a good balance between cost and performances. Price, efficiency, compactness and weight are all an important goal for designers. Thus, Pareto curves allow addressing the problem of multi objectives design [9], where objectives tend to go to opposite directions. These curves represent a set of optimizations based on load specifications and provide a very interesting tool for decision in machine design.

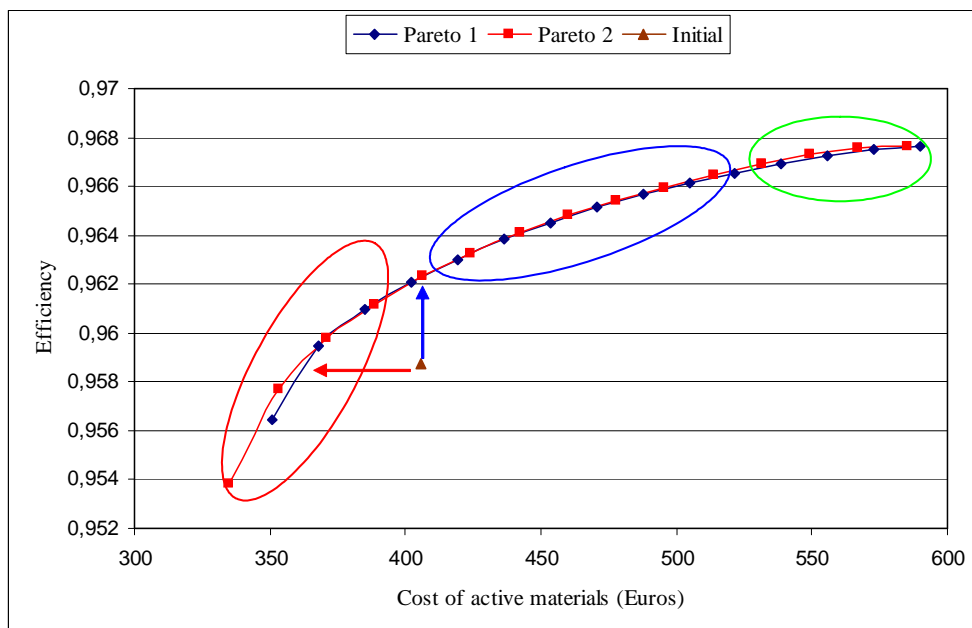


Fig. 8: Pareto curves.

Pareto 1 is achieved with a fixed bore diameter and Pareto 2 with a free bore diameter. Those Pareto curves show 3 zones surrounded in red, blue and green ellipses.

- Red zone: a few increased cost can reach to a sensitive increase of efficiency.
- Blue zone: it is the most important area, efficiency is slightly affected by price increase.
- Green zone: it can be qualified as saturated, because of a slow efficiency increase requires a significant cost increase.

These Pareto curves give us very interesting information:

- For the same cost of active materials, it is possible to build a machine with a more important efficiency and with a better power factor of 0.931, see blue arrow.
- It's possible to build a machine at a lower materials cost with the same performance, see red arrow.

### Range optimizations

Till now, all the achieved optimizations were independently made for each machine, using mono objective optimizations and Pareto curves. But the main objective was to optimize all the range. To reach this goal and in order to have a better understanding of the behaviour of a group of machines, we used a methodology which helped us to optimize all our machines. For a given stator diameter (in order to keep the same housing), we launched the optimization for every speed and stack length of machine. The results led us in every case to a different optimal design of lamination and magnet. Hence at first we made a selection based on the fact that some lamination dimensions were very close. Relaunching this optimization we were able to converge on the optimal lamination for a diameter. Pareto curves give the appropriate tool to choose the definitive machine configuration, with the knowledge of all the impact.

At first, we thought that, to optimize N machines, we would only have to duplicate N times our model. But this methodology showed its limits, because the size of the code to be generated is so important that only one duplication is possible. We have opted for another method which consists in importing the model. This method reduces the number of output constraints (217 against 324 for the duplication method) and the number of the free output parameters is considerably reduced (64 against 1323 for the duplication method). This reduces the size of the code.

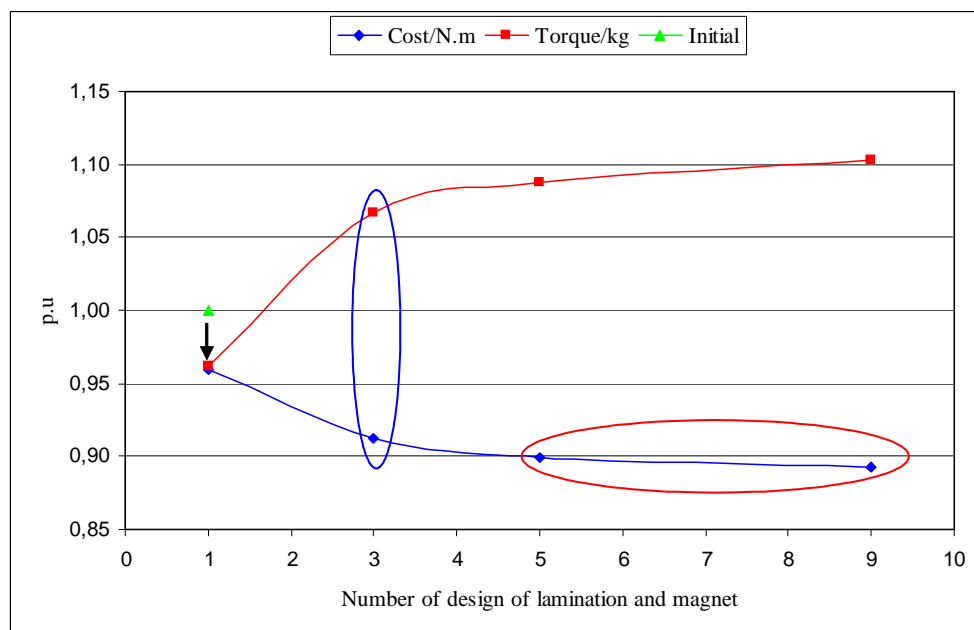


Fig. 9: Pareto curves of range.

We can notice from Pareto curves of range:

- The results obtained with five different laminations are almost identical to those obtained with nine. But the impact in term of cost industrialization is huge (see red ellipse).

- The blue ellipse shows that it is really interesting to have three laminations while optimize the range of motor. Actually, when we reach from 3 to 5 steel laminations we notice that the observed values do not change a lot. On the other hand, we observe sensitive variations when we pass from 1 to 3 different laminations.
- The final solution with one lamination is also interesting (see black arrow). We can clearly show that it is possible to reduce the cost/N.m, but the ratio Torque/kg is lower than the initial design.

### **Conclusions**

In this article we treated the optimization problem of a wide range of machines. For this, we began by establishing an analytical model of the machine (magnetic and thermal). This model was validated experimentally. Considering the number of unknown parameters, an analytical model has been chosen to solve the problem of time-consuming calculations. Then the model was integrated to an optimization tool (CADES). The first optimization results were interesting in terms of the reductions of the materials cost. Finally we have proposed a method to handle the optimization of the motor ranges, the method consists in sharing components (sheet steels stator and rotor, magnets) for several machines. We were able to see that the optimum is not located in N designs for N machines.

### **References**

- [1] B. Delinchant, D. Duret, L. Estrabaut, L. Gerbaud, H. Nguyen Huu, B. du Poux, H.L. Rakotoarison, F. Verdier, F. Wurtz, "An Optimizer using the Software Component Paradigm for the Optimization of Engineering Systems", COMPEL, Vol. 26, Issue 2, pp 368-379, 2007.
- [2] P. Enciu, F. Wurtz, L. Gerbaud, B. Delinchant, "Automatic Differentiation for Electromagnetic Models used in Optimization", COMPEL, (to be published).
- [3] Powell M.J.D., "On the quadratic programming algorithm of Goldfarb and Idnani", Mathematical Programming Study 25, pp 46-61, 1985.
- [4] C.Singh, D. Sarkar, "Practical considerations in the optimization of induction motor design", IEE-PROCEEDINGS-B, Vol. 139, N°4, pp 365-373, July 1992.
- [5] Y. Bertin, "Refroidissement des machines électriques tournantes", Techniques de l'ingénieur, Doc D 3460.
- [6] B. Multon, "Les machines synchrones autopilotées", Préparation à l'agrégation de génie électrique, E.N.S de CACHAN, pp 5, 1993-2004.
- [7] C. Courtel, F. Wurtz, J. Bignon, A comparative study of two methods for constrained optimisation with implicit parameters, Proc. of CEFC98, June 1998, Tucson, USA.
- [8] Olivier Gizolme, Modélisation et Optimisation d'une machine synchrone et de son alimentation pour la traction électrique, Thèse de doctorat, Ecole Centrale de Lyon, 1997, pp 84-85.
- [9] D. Magot, "Méthodes et outils d'aide au dimensionnement. Application aux composants magnétiques et aux filtres passifs", Thèse de doctorat de l'INPG, pp. 54-58, 2004.